AIP Applied Physics Letters

Gigahertz bandwidth electrical control over a dark exciton-based memory bit in a single quantum dot

J. McFarlane, P. A. Dalgarno, B. D. Gerardot, R. H. Hadfield, R. J. Warburton, K. Karrai, A. Badolato, and P. M. Petroff

Citation: Applied Physics Letters **94**, 093113 (2009); doi: 10.1063/1.3086461
View online: http://dx.doi.org/10.1063/1.3086461
View Table of Contents: http://scitation.aip.org/content/aip/journal/apl/94/9?ver=pdfcov
Published by the AIP Publishing

Gigahertz bandwidth electrical control over a dark exciton-based memory bit in a single quantum dot

J. McFarlane,[1,a)] P. A. Dalgarno,[1] B. D. Gerardot,[1] R. H. Hadfield,[1] R. J. Warburton,[1] K. Karrai,[2] A. Badolato,[3] and P. M. Petroff[3]
[1]*School of Engineering and Physical Sciences, Heriot-Watt University, Edinburgh EH14 4AS, United Kingdom*
[2]*Department für Physik, Center for Nanoscience, LMU, Geschwister-Scholl-Platz 1, 80539 Munich, Germany*
[3]*Department of Materials, University of California, Santa Barbara, California 93106, USA*

(Received 17 December 2008; accepted 21 January 2009; published online 6 March 2009)

An optical write-store-read process is demonstrated in a single InGaAs quantum dot within a charge-tunable device. A single dark exciton is created by nongeminate optical excitation allowing a dark exciton-based memory bit to be stored for over ~1 μs. Read-out is performed with a gigahertz bandwidth electrical pulse, forcing an electron spin-flip followed by recombination as a bright neutral exciton, or by charging with an additional electron followed by a recombination as a negative trion. These processes have been used to determine accurately the dark exciton spin-flip lifetime as it varies with static electric field. © *2009 American Institute of Physics*.
[DOI: 10.1063/1.3086461]

Spin is a natural physical quantity for storing and manipulating information in the solid state as a localized spin couples only weakly to the phonons.[1,2] In semiconductor quantum dots, very large spin relaxation times have been demonstrated.[3,4] Spin read-out has been achieved with a spin-to-charge conversion scheme.[5] However, in the case of self-assembled quantum dots, the spin can be created and read-out by exploiting the optical selection rules.[6–8] The selection rules provide a robust link between exciton spin and photon polarization. This is an attractive feature for spin manipulation as radiative recombination is typically a much faster process than spin relaxation. In addition, the use of semiconductor materials allows sophisticated optoelectronic devices to be used. However, spin read-out remains a challenging problem. We present here a proof-of-principle experiment showing how a dark exciton can be converted into a bright exciton within its lifetime, yielding a single photon.

At the heart of our experiment is a device which allows gigahertz control[9,10] over the electron charge trapped in a single quantum dot. Our wafer structure gives us absolute control over the number of electrons in the dot using an applied bias,[11] and a single hole is provided by laser excitation. The device is engineered on a micron length scale in order to reduce the voltage response time such that we can add or remove electrons from the dot on the time scale of exciton recombination (~1 ns). Electrical control over the spin of the neutral exciton is presented here both as a demonstration of single dot gigahertz optoelectronics, and as a potential route to spin storage and read-out.

InGaAs dots were self-assembled within a charge-tunable structure using a Stranski–Krastanov growth method. The dots were grown with a lateral density gradient on top of a 25 nm layer of GaAs (tunneling barrier), beneath which there is a heavily n-doped layer of GaAs (back contact, $n=4\times10^{18}$ cm^{-3}). A 10 nm GaAs capping layer is deposited on top of the dots, followed by a superlattice consisting of 24 AlAs/GaAs pairs to prevent hole tunneling to the metalized top surface (a 5 nm thin semitransparent NiCr Schottky gate). In this way static electric fields applied between the back contact and the Schottky gate control electron tunneling from the back contact through the tunneling barrier into the dots. The dots are small enough that there is a pronounced Coulomb blockade at He temperatures.

Two devices were constructed using low dot density wafer material (<10 dots μm^{-2}). The premise of the design (Fig. 1) was to produce high optical collection efficiency devices with low resistance and capacitance properties such that the dots respond to an applied voltage on a nanosecond timescale. This was achieved by paying attention to four factors. First, the "parallel plate" capacitance formed by the Schottky gate and the back contact was miniaturized by reducing the Schottky gate area to less than 700 μm^2. Second, stray capacitances were minimized by removing unneeded areas of the back contact with a ~400 nm deep wet etch. Third, low resistance macroscopic contacts connect the device to a high speed coaxial cable using low resistance silver conductive paint; a 360 nm thick layer of NiCr connects the Schottky gate to the coax inner, and annealed layers of AuGe/Ni/AuGe (60/10 /60 nm, respectively) form an Ohmic contact between the back contact and the coax outer. Lastly, the connections to the coax were placed more than 1 mm

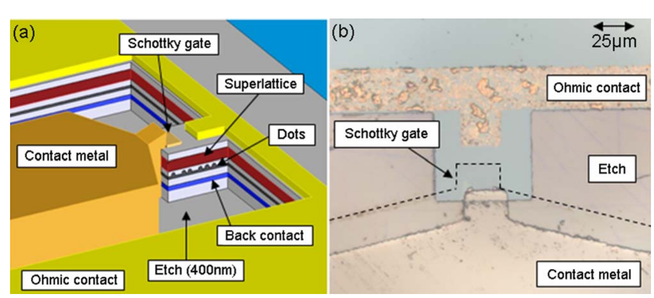

FIG. 1. (Color online) Device 1 (a) schematic (not to scale) and (b) top view optical microscope image (with scaling). Shown are the 5 nm semitransparent Schottky gate, the 400 nm deep wet etch, the Ohmic contact, and the 360 nm thick NiCr electrical contact strip. (a) includes a representation of the AlAs/GaAs superlattice (red), the dot layer (black), and the n-doped back contact (blue).

[a)]Electronic mail: J.McFarlane@hw.ac.uk.

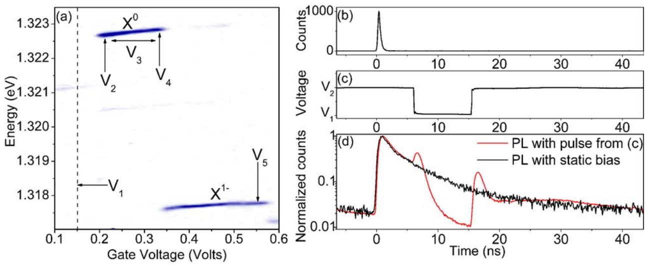

FIG. 2. (Color online) (a) Contour plot showing the PL from a dot in device 1 as a function of the applied bias. Read-out noise on the detector (dot PL >150 counts) is shown as white (dark blue). The labeled parts are the bias point in which only a hole is stored in the dot (V_1), the X^0 plateau extent (V_2 to V_4), and the X^{1-} read-out bias (V_5). The write voltage V_3 can be varied over the X^0 plateau. (b) A time-resolved measurement of the nonresonant laser excitation, the duration of the pulse being determined by the timing jitter of the single photon detector. (c) An oscilloscope measurement of the voltage pulse applied to the sample. (d) TCSPC of X^0 recorded from a dot in device 2 following laser excitation at $t=0$ (b) while a voltage pulse (c) is applied (red), alongside a second plot using a static voltage bias V_2 (black).

away from the optically active area, allowing a superhemispherical solid immersion lens ($n=2.15$) to be placed centrally over the Schottky gate in order to boost the photoluminescence (PL) collection efficiency by a factor of ~5.[12] In device 1 the Ohmic contact is placed 10 μm from the Schottky gate, minimizing the resistance of the device. In device 1 the Ohmic contact, etch, and contact metal dimensions form a coplanar waveguide impedance-matched to the 50 Ω high-speed cabling. In device 2, the Ohmic contact is placed 3 mm from the Schottky gate.

High-speed coaxial cables (<100 ps, 10:90 voltage response time) allow a voltage to propagate from an Agilent 81133A pulse pattern generator (PPG) (60 ps and 10:90 rise time) to the sample at low temperature with subnanosecond rise time. The PL is spectrally dispersed by a blazed grating spectrometer. There are two options for detecting the PL. The first is to record the spectra using a liquid nitrogen-cooled charge-coupled device camera (~50 μeV spectral resolution) positioned at one exit aperture of the spectrometer. The second option utilizes a second exit aperture of the spectrometer allowing a small energy range (~0.5 meV bandwidth) to be coupled into a multimode fiber which leads to a Si-based single photon avalanche detector (SPAD) (~400 ps with full width at half maximum jitter), allowing time correlated single photon counting (TCSPC).

Under 830 nm continuous wave (cw) laser illumination, varying the gate voltage (V_g) and detecting the PL gives a clear picture of the dot charging[11] [Fig. 2(a)]. At low values of V_g (e.g., $V_g=V_1$), the conduction energy levels of the dot are above the Fermi level (defined by the back contact) and an electron in the dot will tunnel out through the tunneling barrier within ~10 ps.[14] A single hole (h) however can be confined in the dot in this bias regime. Hole tunneling is prohibited by the thin capping layer and the blocking barrier. At $V_2<V_g<V_4$, in the presence of a hole, a single electron tunnels into the dot and the Coulomb blockade prevents further electron tunneling, so a neutral exciton (X^0) is formed. In a previous work,[13] a nongeminate exciton creation results in 50% probability of creating either bright or dark X^0. At 0.35 V$<V_g<$0.56 V, a second electron can overcome the Coulomb repulsion from the first electron and tunnel into the dot, creating a negative trion (X^{1-}).

The 10:90 voltage response time of each device was measured using TCSPC of a single dot X^0 PL. Under 830 nm cw illumination, the PPG was connected to the Schottky gate and set to output a 10 MHz square wave with a low voltage of 10 mV below the $h\rightarrow X^0$ charging point and a high voltage of 10 mV above the $X^0\rightarrow X^{1-}$ charging point. The dot is only capable of forming X^0 while V_g experienced by the dot is within the X^0 plateau, which only occurs at the changing edges of the square wave. The time during which PL is recorded at each edge of the square wave can then be considered the V_g rise/fall time experienced by the dot, and represents a measure of the voltage response time of the device. Device 1 (2) has a voltage response time of ~1.6 ns (~4 ns). The larger response time for device 2 relative to device 1 arises from the larger RC time constant, as expected from the fabrication.

A single dot in device 2 was excited by 60 ps optical pulses from an 830 nm laser source [Fig. 2(b)]. TCSPC was performed on PL from X^0 at 1.3133 eV under two separate applied voltages. The first was a static gate voltage set at V_2. The second was a time varying voltage as shown in Fig. 2(c). In the first case [Fig. 2(d), black] a biexponential decay is observed:[13] the fast (1.1 ns) decay arises from recombination of the bright exciton; the slow, (6.6 ns) decay arises from the dark exciton which is incapable of radiative recombination without first experiencing a change in spin from $L=2$ to $L=1$. In this device, the exciton changes its spin via an electron spin-flip, the electron exchanging its spin with the back contact (cotunneling) in order to become bright.[13] Two significant changes are observed when compared with the TCSPC for the second case [Fig. 2(d), red]. First, between $t=8$ ns and $t=16$ ns the PL is suppressed. When the voltage changes to V_1 the electron tunnels out of the dot and the PL is quenched. The reappearance of the PL once the voltage is restored to V_2 shows that the hole is stored throughout. Second, peaks can be seen at 7 and 17 ns. At both edges of the X^0 plateau are voltage regions in which cotunneling is faster than the radiative decay. Within these regions tunneling between the dot and the back contact randomizes the electron spin of the dark exciton, allowing radiative recombination as a bright neutral exciton. As the voltage is changed from V_2 to V_1 the dark-bright spin-flip rate increases, causing the peaks.

The peaks at $t=7$ ns and $t=17$ ns in Fig. 2(d) suggest that dark excitons can be deterministically forced to become bright by using GHz voltage pulses to control the spin-flip lifetime. We confirm this with a write-store-read process with the single dark excitons shown in Fig. 3(c). Two static voltage biases are defined in Fig. 2(a). The first is in the center of the X^0 plateau (V_3) and defines the "write" voltage. The second bias point is in either of the two cotunneling dominated regions (V_2 or V_4) and functions as the "read" voltage. A 60 ps pulse from an 830 nm laser [Fig. 3(a)] nonresonantly creates an X^0 in the dot at time $t=0$ and $V_g=V_3$ [Fig. 3(b)]. The TCSPC of X^0 [Fig. 3(c)] shows a peak at $t=0$ which is due to the fast (~600 ps) radiative recombination of the bright exciton. A secondary slow decay is observed corresponding to the long (~800 ns) spin-flip lifetime of the dark exciton at this voltage. At seven storage values (Δt) the voltage was changed to V_2 or V_4 [Fig. 3(b)], and a PL peak was recorded. Randomization of the electron spin occurs at V_2 and V_4 causing any dark excitons to become bright, allowing recombi-

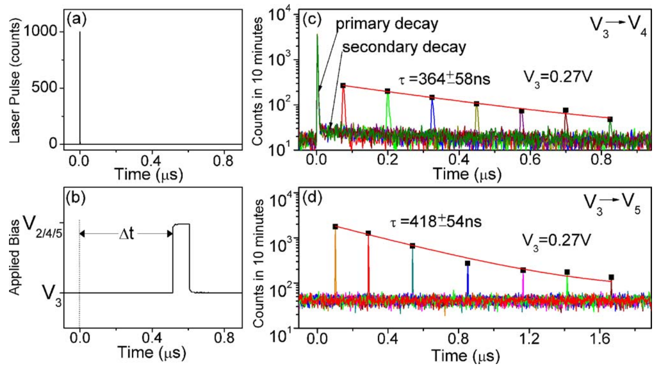

FIG. 3. (Color online) (a) The laser pulse applied to device 1 at $t=0$, measured with a SPAD. (b) An oscilloscope measurement of the voltage pulse applied between the voltages specified in Fig. 2(a) at a particular value of Δt. (c) The PL from X^0 recorded when the laser pulse from (a) and the voltage pulse from (b) between V_3 and V_4 are applied to device 1. (d) The PL from X^{1-} recorded when the laser pulse from (a) and the voltage pulse from (b) between V_3 and V_5 are applied to device 1. The increased background counts in (d) are thought to arise from laser scattering effects within the spectrometer. The peak heights in (c) and (d) are fitted with exponential decays (red lines) in order to find the spin-flip time τ at the point V_3.

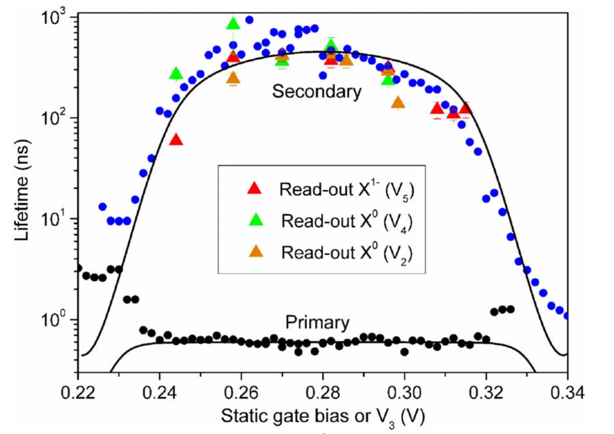

FIG. 4. (Color online) Comparison of X^0 lifetimes taken from the same dot as Fig. 3 in device 1 using the voltage pulsing technique (red, green and orange triangles) with that of standard TCSPC (black and blue circles). The effect of cotunneling can be seen as a rapid decrease in secondary lifetime toward either edge of the $X0$ plateau. Included is a fit (black line) based on exciton spin-flip via electron tunneling (see Ref. 13) using $\tau_t=26$ ps, $\delta_{BD}=0.263$ meV, $T=5$ K, $\gamma_r=1.67$ ns^{-1}, and $\gamma_{nr}=0$ ns^{-1}.

nation within ~1 ns. This method has been successful with measured Δt of over 1.5 μs.

A second write-store-read method again involves creating X^0 in the dot nonresonantly with a 60 ps pulse of 830 nm laser light at $t=0$ and $V_g=V_3$ [Fig. 3(a)]. In this case however, the read-out process involves converting a dark X^0 into an X^{1-}. The dark exciton is stored for seven different Δt and the PPG is used to apply a voltage pulse from V_3 to V_5 [Fig. 3(b)] causing the appearance of an X^{1-} PL peak [Fig. 3(d)]. At $t=\Delta t$ the change in voltage causes a second electron to tunnel into the dot from the back contact, forming an X^{1-}. Unlike X^0, X^{1-} has no fine structure and is able to recombine radiatively in ~700 ps, giving a distinct read-out signal.

We can fit an exponential decay [Figs. 3(c) and 3(d), red lines] to the peaks in PL signal versus decay time. The fit gives a value for the electron spin-flip time τ of a dark exciton at voltage V_3. The advantage of the pulsed voltage experiment is that all the signal at $t>\Delta t$ in the dc experiment is bundled into one small time window, enhancing the accuracy with which τ can be determined. By varying V_3 across the bias extent of the neutral exciton we show in Fig. 4 that the τ values obtained closely follow the secondary lifetime of X^0 taken with static voltage bias. The dependence of τ on V_3 can be understood by calculating the cotunneling rate from the Anderson Hamiltonian.[13] The model is parameterized with the electron tunneling time (τ_t), the X^0 energy splitting between dark and bright states (δ_{BD}), the temperature (T), and the radiative (γ_r) and nonradiative (γ_{nr}) decay rates. The model provides a good fit as shown in Fig. 4. In particular, a nonradiative decay rate is not required ($\gamma_{nr}=0$ ns^{-1}) and there is a 50:50 relative intensity between the primary and secondary decay in the center of the X^0 extent. This confirms that the X^0 secondary lifetime is limited by cotunneling even at the plateau center, in contrast to Ref. 13, where there is a nonradiative decay rate. This is due to the increased capping layer thickness of the wafer in Ref. 13; hole tunneling from the dot into the capping layer provides a nonradiative decay path for the neutral exciton.[14] In this particular device, dark exciton spin relaxation is always dominated by cotunneling. However, by increasing the tunneling barrier, cotunneling can be suppressed by many orders of magnitude,[15] and it will be difficult to measure the dark exciton spin relaxation via a decay curve. Instead, spin read-out with a gigahertz bandwidth pulse is much more suitable.

In conclusion we have demonstrated that gigahertz bandwidth voltage pulses can be applied over a charge-tunable single quantum dot device to manipulate the charge of an exciton deterministically within its recombination lifetime. Using this method, single dark excitons have been used as bit memory elements. Optical read-out is carried out by converting the dark X^0 into a bright X^0 (emission at X^0 wavelength) or into an X^{1-} (emission at X^{1-} wavelength). This technique offers great potential for a deterministic single photon source in which individual photons are generated with a gate voltage pulse, and for hole spin read-out.

[1]R. Hanson, L. P. Kouwenhoven, J. R. Petta, S. Tarucha, and L. M. K. Vandersypen, Rev. Mod. Phys. **79**, 1217 (2007).
[2]R. Hanson and D. D. Awschalom, Nature (London) **453**, 1043 (2008).
[3]M. Kroutvar, Y. Ducommun, D. Heiss, M. Bichler, D. Schuh, G. Abstreiter, and J. J. Finley, Nature (London) **432**, 81 (2004).
[4]S. Amasha, K. MacLean, I. P. Radu, D. M. Zumbühl, M. A. Kastner, M. P. Hanson, and A. C. Gossard, Phys. Rev. Lett. **100**, 046803 (2008).
[5]J. M. Elzerman, R. Hanson, L. H. Willems van Beveren, B. Witkamp, L. M. K. Vandersypen, and L. P. Kouwenhoven, Nature (London) **430**, 431 (2004).
[6]M. Atatüre, J. Dreiser, A. Badolato, A. Högele, K. Karrai, and A. Imamoglu, Science **312**, 551 (2006).
[7]M. Atatüre, J. Dreiser, A. Badolato, and A. Imamoglu, Nat. Phys. **3**, 101 (2007).
[8]J. Berezovsky, M. H. Mikkelsen, O. Gywat, N. G. Stoltz, L. A. Coldren, and D. D. Awschalom, Science **314**, 1916 (2006).
[9]S. Strauf, N. G. Stoltz, M. T. Rakher, L. A. Coldren, P. M. Petroff, and D. Bouwmeester, Nat. Photonics **1**, 704 (2007).
[10]Z. Yuan, B. E. Kardynal, R. M. Stevenson, A. J. Shields, C. J. Lobo, K. Cooper, N. S. Beattie, D. A. Ritchie, and M. Pepper, Science **295**, 102 (2002).
[11]R. J. Warburton, C. Schäflein, D. Haft, F. Bickel, A. Lorke, K. Karrai, J. M. Garcia, W. Schoenfeld, and P. M. Petroff, Nature (London) **405**, 926 (2000).
[12]V. Zwiller and G. Björk, J. Appl. Phys. **92**, 660 (2002).
[13]J. M. Smith, P. A. Dalgarno, R. J. Warburton, A. O. Govorov, K. Karrai, B. D. Gerardot, and P. M. Petroff, Phys. Rev. Lett. **94**, 197402 (2005).
[14]P. A. Dalgarno, J. McFarlane, B. D. Gerardot, R. J. Warburton, K. Karrai, A. Badolato, and P. M. Petroff, Appl. Phys. Lett. **89**, 043107 (2006).
[15]J. Dreiser, M. Atatüre, C. Galland, T. Müller, A. Badolato, and A. Imamoglu, Phys. Rev. B **77**, 075317 (2008).